Macromolecular Research, Vol. 22, No. 12, pp 1320-1329 (2014)
DOI 10.1007/s13233-014-2183-x

www.springer.com/13233
pISSN 1598-5032 eISSN 2092-7673

Dual Growth Factor-Loaded Core-Shell Polymer Microcapsules Can Promote Osteogenesis and Angiogenesis

Ramesh Subbiah[1,2], Ping Du[1,2], Mintai Peter Hwang[2], In Gul Kim[2], Se Young Van[1,2], Yong Kwan Noh[2,3], Hansoo Park[4], and Kwideok Park*[,1,2]

[1]*Department of Biomedical Engineering, Korea University of Science and Technology (UST), Daejon 305-350, Korea*
[2]*Center for Biomaterials, Korea Institute of Science and Technology (KIST), Seoul 136-130, Korea*
[3]*Department of Biomedical Engineering, School of Medicine, Kyunghee University, Seoul 130-701, Korea*
[4]*School of Integrative Engineering, Chung-Ang University, Seoul 156-071, Korea*

Received July 4, 2014; Revised August 5, 2014; Accepted August 26, 2014

Abstract: Growth factors (GFs) are very critical in stem cell differentiation and tissue regeneration. Therefore GF delivery carriers have been a major subject in tissue engineering research. In this study, we prepare and optimize core-shell microcapsules (C-S MCs) for dual GF delivery. The C-S MCs, composed of an alginate shell and poly(lactic-*co*-glycolic) acid (PLGA) core, are fabricated using an electrodropping method *via* custom-made coaxial needles. They are 198±38 μm in diameter with an average core size of 90±13 μm, and they are fabricated using an alginate concentration of 1% (w/v), an electrical voltage of 11 kV, and an inner syringe flow rate of 50 μL/min. Using this platform, dual GFs, bone morphogenetic protein (BMP-2) and vascular endothelial growth factor (VEGF) are encapsulated in the alginate shell and PLGA core, respectively. *In vitro* release tests of dual GF-loaded C-S MCs reveal early release of BMP-2, followed by VEGF on a temporal release profile of 28 days. *In vitro* study of the dual GF-loaded MCs demonstrates their osteogenic activity with preosteoblasts; osteogenic markers (osteocalcin and type I collagen) are upregulated and both calcium content and alkaline phosphatase (ALP) activity also increased. In addition, C-S MCs combined with collagen and preosteoblasts were subcutaneously transplanted to the dorsal region of nude mice for 3 weeks. Analysis of the retrieved constructs exhibits that both osteogenesis and angiogenesis were more active in the group containing dual GF-loaded MCs, along with deep penetration of blood vessels inside the construct, compared to blank MCs or single GF (BMP-2)-loaded MCs. This study proposes a dual GF delivery carrier using C-S MCs and demonstrates the feasibility of C-S MCs in the induction of osteogenesis and angiogenesis.

Keywords: core-shell microcapsules, dual growth factor delivery, electrodropping, osteogenesis, angiogenesis.

Introduction

Eliciting the differentiation of stem cells into a particular lineage is a crucial prerequisite for tissue repair and regeneration.[1-3] Multiple signaling cues have been implicated, including those of biochemical (growth factors; GFs), biophysical (topography), and biomechanical (elastic modulus) ones.[2,4] While biophysical and biomechanical factors are contact-mediated and generally derived from the environmental niche and its attributes,[2] biochemical cues impart signals in a different manner; non-contact-mediated paracrine signaling and surface-bound (contact-mediated) signaling. Thus, both appropriate selection of GFs and their time-dependent controlled delivery of such GFs to target sites are a major interest in the study of stem cells and tissue regeneration. The conventional use of single GF bolus delivery has been partially successful in tissue regeneration, due mostly to uncontrolled release of GFs.[5] Consequently, many carrier systems for the localized and controlled delivery of a single GF have been explored and expanded further to the use of multiple GFs.[6-9] Several groups have proven the importance of dual GF delivery in the regeneration of complex tissues.[5,10-13] In particular, the temporally controlled delivery of dual GFs for stem cells differentiation has been extensively investigated. Since Richardson *et al.* demonstrated the use of a dual growth factor, such as vascular endothelial growth factor (VEGF) and platelet-derived growth factor (PDGF) in a polymer scaffold-based delivery system for angiogenesis,[5] others have adopted the concept of sequential dual GF delivery for a wide variety of tissue engineering applications including angiogenesis,[11] neurogenesis,[10] osteogenesis,[13,14] myogenesis,[15] and chondrogenesis.[16]

In this study, we propose a core-shell microcapsule (C-S MC)

*Corresponding Author. E-mail: kpark@kist.re.kr

for dual GF delivery. Electrospinning offers a rapid method in the production of such C-S MCs.[11,17-20] While employing a custom-made coaxial and non-coaxial syringe system, electrodropping system is capable of generating a homogenous distribution of C-S MCs in size and shape.[18] Since C-S MCs hold core and shell domain, respectively it is expected that their biggest advantage is the temporally controlled release of individual GFs, each with a different release profile.[11] In addition to the fabrication method, the type of polymers used is important with regards to processability; alginate, a natural biopolymer and poly(lactic-*co*-glycolic) acid (PLGA), a Food and Drug Administration (FDA)-approved synthetic polymer are preferred.[21-24] In this work, by tailoring the loading formulation and fabrication parameters, bone morphogenetic protein (BMP-2) and vascular endothelial growth factor (VEGF) are encapsulated in the alginate shell and PLGA core, respectively. The dual GF-loaded C-S MCs were subsequently evaluated for *in vitro* osteogenic differentiation of preosteoblasts. Furthermore, C-S MCs and preosteoblasts are embedded together within a collagen scaffold and subcutaneously transplanted into nude mice to investigate both biocompatibility of the C-S MCs and their osteogenic and angiogenic potential *in vivo*.

Experimental

Preparation and Optimization of Core-Shell Microcapsules (C-S MCs). C-S MCs were prepared by using PLGA emulsion (core) and alginate solution (shell), respectively (Figure 1(A)). A PLGA emulsion was prepared using a double emulsion evaporation method, in which 6% (w/v) PLGA (75:25, RG 757S, MW: 270,000; Boehringer Ingelheim, Germany) in chloroform was loaded into a glass vial containing an aqueous phase of 5% (w/v) polyvinyl alcohol (PVA; 87-89% hydrolyzed, MW 13,000-23,000). The immiscible organic and aqueous solutions were then sonicated for 2 min using a probe tip sonicator (Sonic Dismembrator Model 500, Fisher Scientific) to yield a milky emulsion. 5,000 ng of VEGF (R&D System; Minneapolis, MN) was subsequently added to the emulsion, which was subjected to 10 s of mild sonication for further homogenous mixing. Meanwhile the shell region of MCs was prepared by mixing 1:1 (v/v) ratio of aqueous sodium alginate solution (0.025% to 1% w/v; 300-400 cp; Wako Chemicals, Osaka, Japan) and an ethylene glycol (Sigma-Aldrich, St. Louis, MO) solution loaded with 5,000 ng of BMP-2 (R&D System; Minneapolis, MN). Bovine serum albumin (BSA; Sigma-Aldrich, St. Louis, MO) was added as a stabilizing agent for GFs in the preparation of both polymers. As shown in Figure 1, MCs were produced using a slightly modified protocol based on our previous report.[11] A plastic (18G) and stainless steel (26G) nozzle was employed as an outer and inner nozzle, respectively, in which the inner nozzle was spatially positioned in the center of the outer nozzle with the use of copper coil (Figure 1(B),(C)). The PLGA emulsion and sodium alginate solution are separately injected

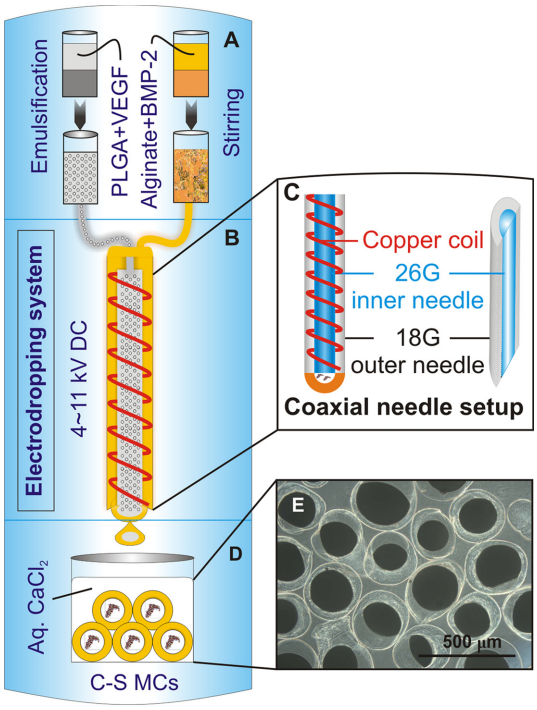

Figure 1. An experimental schematic of fabrication procedure of C-S MCs. (A) BMP-2-loaded PLGA emulsion is prepared using an ultrasonication-assisted emulsification method while VEGF-loaded alginate is prepared *via* a simple stirring method. (B) A custom-made coaxial needle is employed with an electrodropping system for the fabrication of C-S MCs. (C) A detailed coaxial needle set-up with a copper coil. (D) Formation of C-S MCs crosslinked in $CaCl_2$ solution. (E) Optical microscopic images of C-S MCs (Scale bar: 500 μm).

into the system using a microsyringe pump; the flow rate was adjusted to 120 μL/min for alginate and 80 μL/min for PLGA emulsion. The high electric voltage was applied ranging from 4 to 11 kV. The distance between the nozzle tip and the grounded collector was 10 cm. The electrodropping system (NanoNC, eS-robot electrospinning spray system, Seoul, Korea) produces C-S MC droplets, which were subsequently solidified in 1% $CaCl_2$ solution (w/v) (Figure 1(D),(E)). The C-S MCs were washed in 2.5% PVA solution (w/v), followed by deionized water (DW), and finally filtered using a 100 mm nylon cell strainer (BD Falcon™, Franklin Lakes, NJ). C-S MCs were then stored in a glass vial at 4 °C for future use.

Characterization. The morphology of PLGA emulsion and alginate domain was analyzed individually in a contact mode using a bio-atomic force microscope (Bio-AFM, Nanowizard II, JPK Instruments, Berlin, Germany) equipped with a HYDRA2R-50NG AFM probe (AppNano). For each sample preparation, PLGA emulsion was spin-coated on a fresh mica substrate whereas a drop of solution containing C-S MCs was placed on a glass substrate. They were then dried in vacuum oven at 37 °C prior to AFM imaging. The scan sizes are 10×10, 40×40, and 100×100 μm, respectively. The root mean

square (RMS) roughness (R_q) was subsequently determined using analytical software (JPK Data Processing). The average size of PLGA nanoparticles (NPs) and distribution were also analyzed using a laser diffraction particle sizer (Malvern Mastersizer 2000, Malvern, UK).

Release Test of C-S MCs. Release test of C-S MCs was carried out *in vitro* with MCs containing VEGF in the core and BMP-2 in the shell. During the fabrication of dual GF MCs, VEGF (2 μg) was mixed in PLGA (6%, w/v) solution, supplemented with BSA (4.5%, w/v) and PVA (5%, w/v), then followed by a brief sonication for 30 s. BMP-2 (2 μg) dissolved in BSA (4.5%, w/v) was added in alginate solution (300-400 cp). The prepared MCs were weighed in 20 μg, placed in a vial containing DW, and incubated at 37 °C for 28 days. The whole volume of DW was collected at the predetermined times and fresh one was then replenished. When the released amount of each GF was determined at specific time points using enzyme-linked immunosorbent assay (ELISA; R&D Systems) kit, the cumulative percent release of each GF was calculated and plotted on a temporal basis.

Induction of Osteogenesis of Preosteoblasts *In vitro*. Preosteoblasts were seeded at a density of 2×10^4 cells/cm^2 on either plastic or glass coverslips, and cultured in minimum essential medium alpha (α-MEM) supplemented with 10% fetal bovine serum (FBS) and 1% penicillin/streptomycin (P/S; Gibco BRL, Grand Island, MD). To investigate osteogenic potential of C-S MCs *in vitro*, cells are cultured in osteogenic media that consist of α-MEM supplemented with 10% FBS, 1% P/S, 10 mM β-glycerophosphate, 0.1 μM dexamethasone, and 50 μg/mL L-ascorbic-2-phosphate. There are three test groups: negative control (G1: culture without BMP-2), positive control (G2: culture with soluble BMP-2), and dual GF (VEGF/BMP-2)-loaded MCs (G3: culture in osteogenic medium without BMP-2). C-S MCs that contain no GFs were placed in a transwell insert, with the preosteoblasts on the bottom plate, and incubated for 2 weeks with (G2) or without soluble BMP-2 (G1) in the osteogenic medium. Dual GF-loaded MCs followed the same format. The medium was changed every 3 days and cell culture was carried out under a standard culture condition (37 °C and 5% CO_2).

Measurement of Alkaline Phosphatase (ALP) Activity and Calcium Content. Both ALP activity and calcium content were determined to assess the osteogenic potential of C-S MCs. After 14 days of culture, preosteoblasts were treated with 0.5% Triton X-100 solution, collected *via* scraping, and vortexed for approximately 30 min. ALP activity was then evaluated using an ALP kit (LabAssay, Wako Pure Chemicals, Japan) following the manufacturer's instructions; aliquots (5 μL) of each sample were transferred to a 96-well plate, supplemented with a working reagent (200 μL), incubated for 3 min at RT, and measured for absorbance at 405 nm using a micro plate reader (Thermo Scientific). Additionally, calcium content was also quantified using a QuantiChrom Calcium Assay Kit (DICA-500, BioAssay systems, USA) following the manufacturer's instructions. Total protein amounts as determined using a bicinchoninic acid (BCA) assay kit (Pierce) were used to normalize the ALP activity of each group.

Immunofluorescence Staining (IFS) of Osteogenic Protein Markers. Expression of both osteocalcin (OCN) and type I collagen (Col I) was also investigated after 2-week culture of preosteoblasts. The samples were fixed in 4% ρ-formaldehyde, washed with phosphate buffered saline (PBS), treated with peroxo-block solution for 1 min, and washed with PBS several times. They were then permeabilized with 0.1% Triton X-100 for 5 min, blocked with 3% BSA for 2 h, and incubated with the primary antibodies at 4 °C overnight; rabbit anti-OCN and goat anti-Col I antibodies diluted in 1% BSA (1:50). These samples were then incubated for 1 h at room temperature with corresponding secondary antibodies; Alexa Fluor 488-conjugated goat anti-mouse IgG and Alexa Fluor 594-conjugated donkey anti-goat IgG, respectively diluted in 1% BSA (1:200). The immunostained samples were further subjected to DAPI staining for nucleic staining of cells. Fluorescent signals of the target proteins were visualized *via* a confocal microscopy (Olympus FluoView FV1000, Tokyo, Japan).

Subcutaneous Transplantation of Collagen/C-S MCs Constructs. A collagen scaffold was used to fabricate a construct including C-S MCs in evaluating osteogenesis of preosteoblast *in vivo*. Type I collagen was extracted from rat tail, lyophilized, and dissolved in 0.1% acetic acid following a standard protocol.[25] A stock solution of collagen was prepared at the concentration of 1.5% w/v, which was further diluted and neutralized with buffer solutions (1x M199 (Lonza), 10x M199, and 1 M NaOH) on ice prior to the scaffold fabrication. VEGF/BMP-2-loaded C-S MCs were homogeneously mixed with 0.3% (w/v) collagen solution in ice bath to prevent the gelation of collagen, and followed by the addition of preosteoblasts (1×10^6). The constructs were subsequently transferred to 96-well plate and incubated at 37 °C for 30 min to allow crosslinking of collagen. Three experimental groups were prepared: C-S MCs without GFs (G1), C-S MCs with single GF (BMP-2) (G2), and C-S MCs with dual GFs (G3). These constructs were incubated in an osteogenic medium for 24 h before subcutaneous implantation. Nude mice (8-week old male) were anesthetized *via* intraperitoneal injection of a mixture of Zoletil and Rompun (1 mL/kg), subsequently transplanted with each construct (5.5±0.3 mm diameter) (n=4, each) in the subcutaneous dorsal region, and sutured using absorbable Vicryl. The animals were euthanized by cervical dislocation after 3 weeks and the transplants were retrieved and fixed in 10% buffered formalin before further analysis.

Histology, Scanning Electron Microscopy (SEM) and IFS. After fixation of the retrieved constructs, they were dehydrated, embedded in paraffin, and serially sectioned in 5 mm thickness. Thin sections were subjected to hematoxylin and eosin (H&E) and *von Kossa* staining, respectively. For *von Kossa* staining, the samples were immersed in a 5% $AgNO_3$

solution under ultraviolet light for 1 h, treated with sodium carbonate/formaldehyde for 1 min, and reacted with a 5% $Na_2S_2O_3$ solution for 5 min. The samples were then rinsed with distilled water, serially dehydrated in ethanol (50%, 75%, 100%), and air-dried. Calcium deposits appear as black or brownish-black spots when examined using an optical microscopy. In addition, to examine the blood vessels formation within the constructs, the sectioned samples were dehydrated through a graded series of ethanol, dried, sputter-coated with platinum, and then mounted onto a scanning electron microscope (SEM; Phenom G2 pro desktop, Eindhoven, Netherlands). Meanwhile, to investigate the synthesis of an osteogenic marker (osteocalcin; OCN) and an angiogenic marker (α-smooth muscle actin; *α*-SMA), the retrieved constructs were transferred into a cryomold containing optimum cutting temperature (OCT) compound solution and frozen with liquid nitrogen. After solidification, the cryomolds were dried with kim-wipes and stored at -80 ºC until further processing. Routine cryosectioning was performed at -21 ºC on frozen blocks using a cryostat (Leica CM 1850). For each block, 5 μm-thick cross-sections were collected along the vertical plane of the construct, washed, and air-dried. After blocking for endogenous peroxidase activity with H_2O_2 diluted in water, samples were demasked *via* treatment with antigen retrieval reagents for 75 min at 98 ºC, followed by blocking with 3% bovine serum albumin (BSA, Sigma) in PBS for 1 h. For OCN staining, samples were incubated with rabbit polyclonal anti-OCN antibody (ab93876) diluted in 1% BSA (1:50) at 4 ºC overnight, followed by reaction with Rhodamine Red-X goat anti-rabbit IgG (R6394) diluted in 1% BSA (1:200) at RT for 1 h. Additionally, the presence of angiogenic marker was also assessed by incubating samples with mouse monoclonal anti-*α*-SMA (A2547; Sigma) diluted in 1% BSA (1:50) at 4 ºC overnight, followed by reaction with donkey anti-mouse IgG H&L Alexa Fluor 555 (ab150106) diluted in 1% BSA (1:500) at RT for 1 h. All samples were washed with PBS three times before incubation with the appropriate secondary antibody. Fluorescence images of the target proteins were observed *via* confocal laser scanning microscopy (Olympus FluoView FV1000, Tokyo, Japan). OCN- and *α*-SMA- positive areas were subjected to threshold processing and analyzed using the

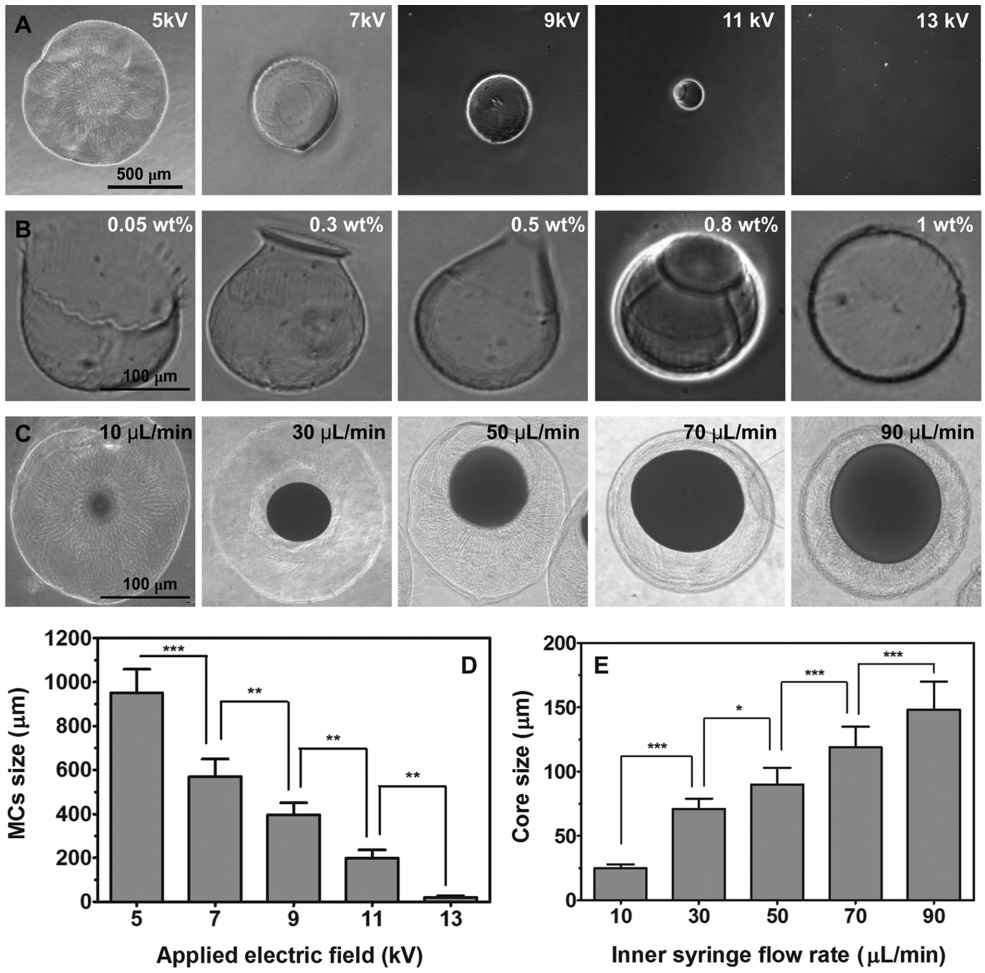

Figure 2. Optimization of C-S MCs. (A) Effect of electrical field on C-S MCs formation (scale bar: 500 μm), An increase in the applied voltage decreases the size of the alginate MC. (B) effect of alginate concentration (scale bar: 100 μm), (C) effect of inner syringe flow rate (scale bar: 100 μm), quantitative comparison of electrical field effect (D), and inner syringe flow rate (E).

area measurement tool function of Image J (NIH). We analyzed six randomly selected non-adjacent cross-section samples in 4 animal groups.

Statistical Analysis. All data presented was obtained from three independent samples, each analyzed in triplicate. A one-way analysis of variance (ANOVA) was conducted using statistical software (GraphPad Prism 5). Statistical significance was determined as *(p<0.05), **(p<0.01), and ***(p<0.001).

Results and Discussion

Core-Shell Microcapsules (C-S MCs) Preparation and Optimization. C-S MCs are fabricated *via* an electrodropping system that utilizes a custom-made coaxial needle.[11] PLGA emulsion prepared *via* ultrasonication-assisted double emulsification[26] and alginate solution are integrated into a C-S MCs (Figure 1). Here, we investigated the effect of various parameters on the morphology of the resulting C-S MCs. In fact, the concentration of alginate solution and the strength of electric field play an important role in generating homogenous MCs. Also, the inner syringe flow rate containing the PLGA emulsion can be tuned to manipulate the size of the MC core. With an increase in the electric field strength, we found a significant decrease in the C-S MC size (Figure 2(A),(D)). It is notable that sprayed particles or broken fibers resulted at an electric field more than 12 kV. Changing the concentration of alginate solution, on the other hand, affected the overall C-S MC morphology, producing various shapes (Figure 2(B)). Finally, we observed that increasing the inner syringe flow rate yielded MCs with a larger core size (Figure 2(C),(E)). MCs did not form with an excessive inner syringe flow rate greater than 110 μL/min; an inner flow rate between 60 to 80 μL/min appears optimal.

C-S MCs Characterization. C-S MCs (fabricated using 1% (w/v) alginate, an inner syringe flow rate of 80 μL/min, and an electric field of 11 kV) are prepared with a core containing VEGF and a shell carrying BMP-2. The GF-loaded C-S MCs consist of a clearly delineated PLGA core and an alginate shell (Figure 3(A)), and form a homogenous population of spherical structures with an average diameter of 198±38 μm. In addition, as assessed *via* atomic force microscopy (AFM) the morphology and topography of the alginate shell surface is a moderately rough, with an average RMS value of 2.3 μm and a surface charge of -24.5 mV (Figure 3(B)). When the roughness and size of the PLGA core of MCs is also analyzed, the PLGA core holds a lot of PLGA nanoparticles (NPs), as shown in AFM image (Figure 3(C)). The average size of NPs is 88±29 nm. Meanwhile, an examination of the release profile indicates a burst release of BMP-2 for the first 3 days (21.6±3.4%), followed by a continuous release (Figure 3(D)). On the other hand, the PLGA core results in a moderate release of VEGF for the first 10 days, followed by

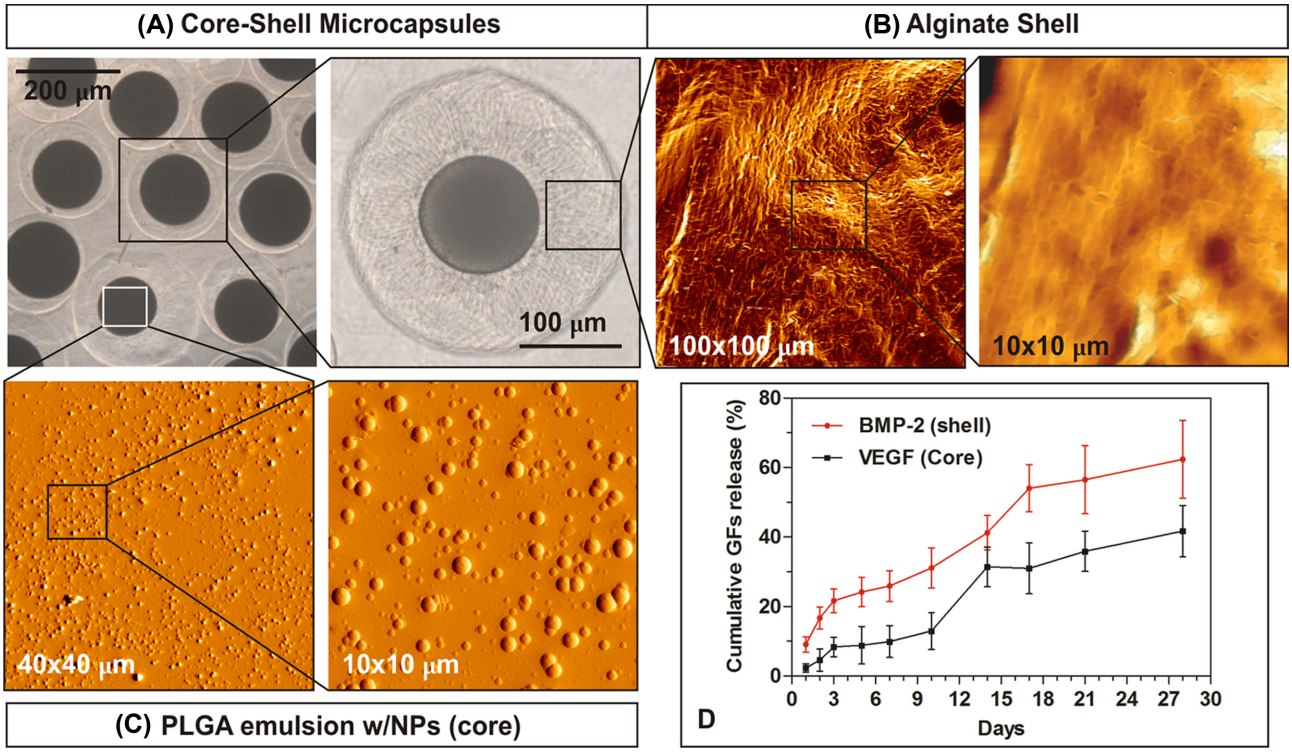

Figure 3. Characterization of C-S MCs. (A) Optical images of a homogenous population of spherical C-S MCs (left: 200 μm; right: 100 μm), (B) 3D height images of the crosslinked alginate shell surface assessed *via* AFM. (C) 3D height images of PLGA core, with a lot of nanoparticles as taken *via* AFM, and (D) *in vitro* release test of growth factors from C-S MCs (n=3) for 28 days.

a sudden rise of release from days 10 to 14. The positional advantage of PLGA core in the C-S MCs would contribute to suppressing the temporal release of protein (VEGF) when compared to that (BMP-2) in the alginate shell, resulting in the early release of BMP-2 from the alginate shell and a delayed release of VEGF from the core.

Induction of Osteogenic Differentiation of Preosteoblasts *In vitro*. The bioactivity of the releasate from the dual GF-loaded C-S MCs is assessed *in vitro* by examining the level of osteogenesis in preosteoblasts. Preosteoblasts, cultured in osteogenic media, are treated with one of the followings: osteogenic media without BMP-2 (G1; negative control), with soluble BMP-2 (G2; positive control), and with BMP-2/VEGF (G3). After 14 days, osteogenic marker proteins are detected *via* immunofluorescence (IFS) that indicates the presence of osteocalcin (OCN) and type I collagen (Col I) in G2 and G3 group (Figure 4(A)). Additionally each group is quantitatively assessed for total protein concentration, calcium content and ALP activity. *In vitro* quantitative results at day 14 suggest a similar level of total protein content (Figure 4(B)) and much higher calcium content in G2 and G3 compared to that of G1 (Figure 4(C)). Normalized by each total protein content, measurement of ALP activity on day 14 indicates a significantly higher amount of ALP in G2 and G3 than that in G1, where the ALP activity is comparable between G3 (BMP-2/VEGF) and G2 (BMP-2) (Figure 4(D)). These results hint that dual delivery of BMP-2 and VEGF *via* C-S MCs can promote an osteogenic differentiation of preosteoblast *in vitro*.

Osteogenesis and Angiogenesis Using Dual GF-Loaded MCs *In vivo*. The sequential delivery of growth factors is recognized very critical in the effective repair of the damaged tissue throughout the course of regeneration.[10,27] In conjunc-

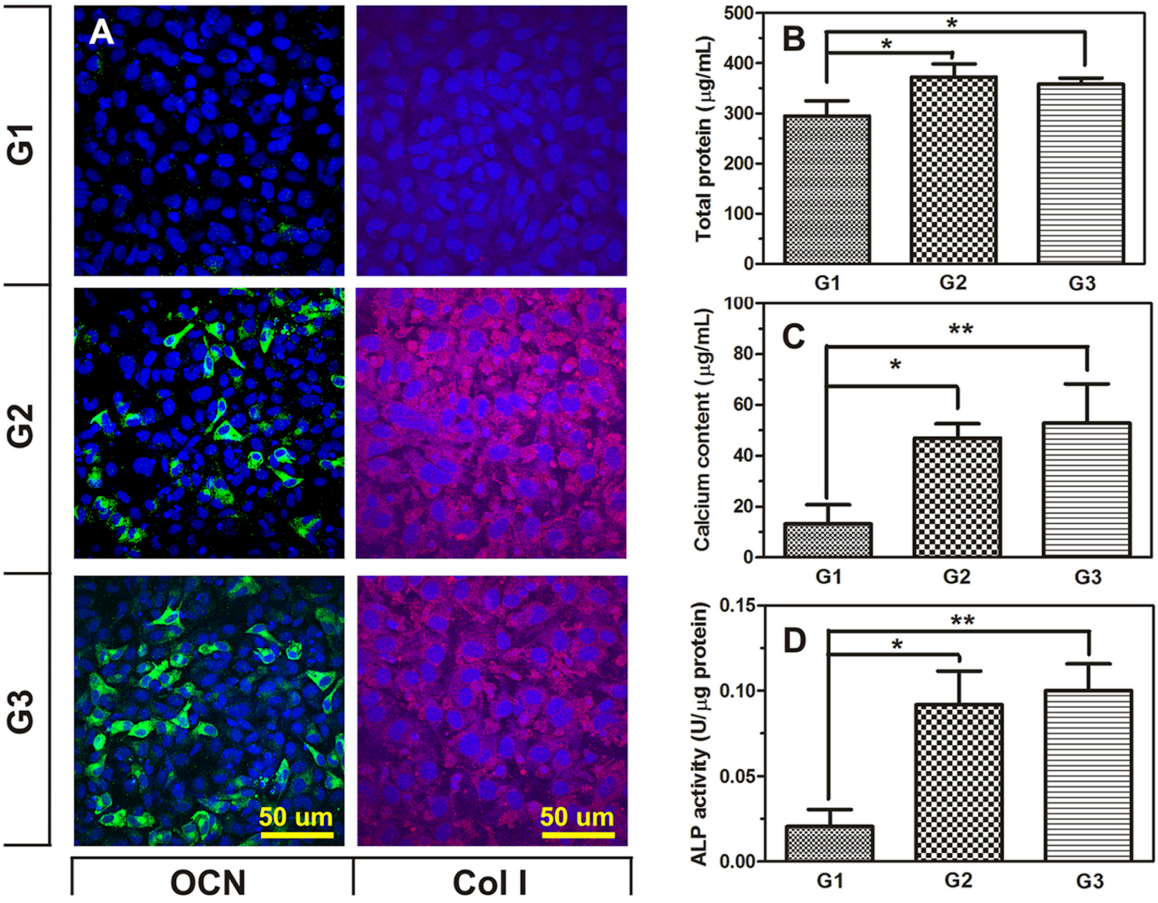

Figure 4. Induction of osteogenic differentiation of preosteoblast *in vitro*. There are three test groups: negative control (G1: culture without BMP-2), positive control (G2: culture with soluble BMP-2), and dual GF (VEGF/BMP-2)-loaded MCs (G3: culture in osteogenic medium without BMP-2). C-S MCs that contain no GFs were placed in a transwell insert, with the preosteoblasts on the bottom plate, and incubated for 2 weeks with (G2) or without soluble BMP-2 (G1) in the osteogenic medium. Dual GF-loaded MCs followed the same format. (A) IFS of osteogenic marker proteins: OCN (green) and Col I (red), along with DAPI nuclear staining (blue), scale bar: 50 μm, (B) total protein concentration as determined by BCA assay, (C) calcium content as quantified *via* Quantichrom calcium assay, (D) measurement of ALP activity as normalized using the total protein of each group. Statistical significance is shown as *(p<0.05) and **(p<0.01).

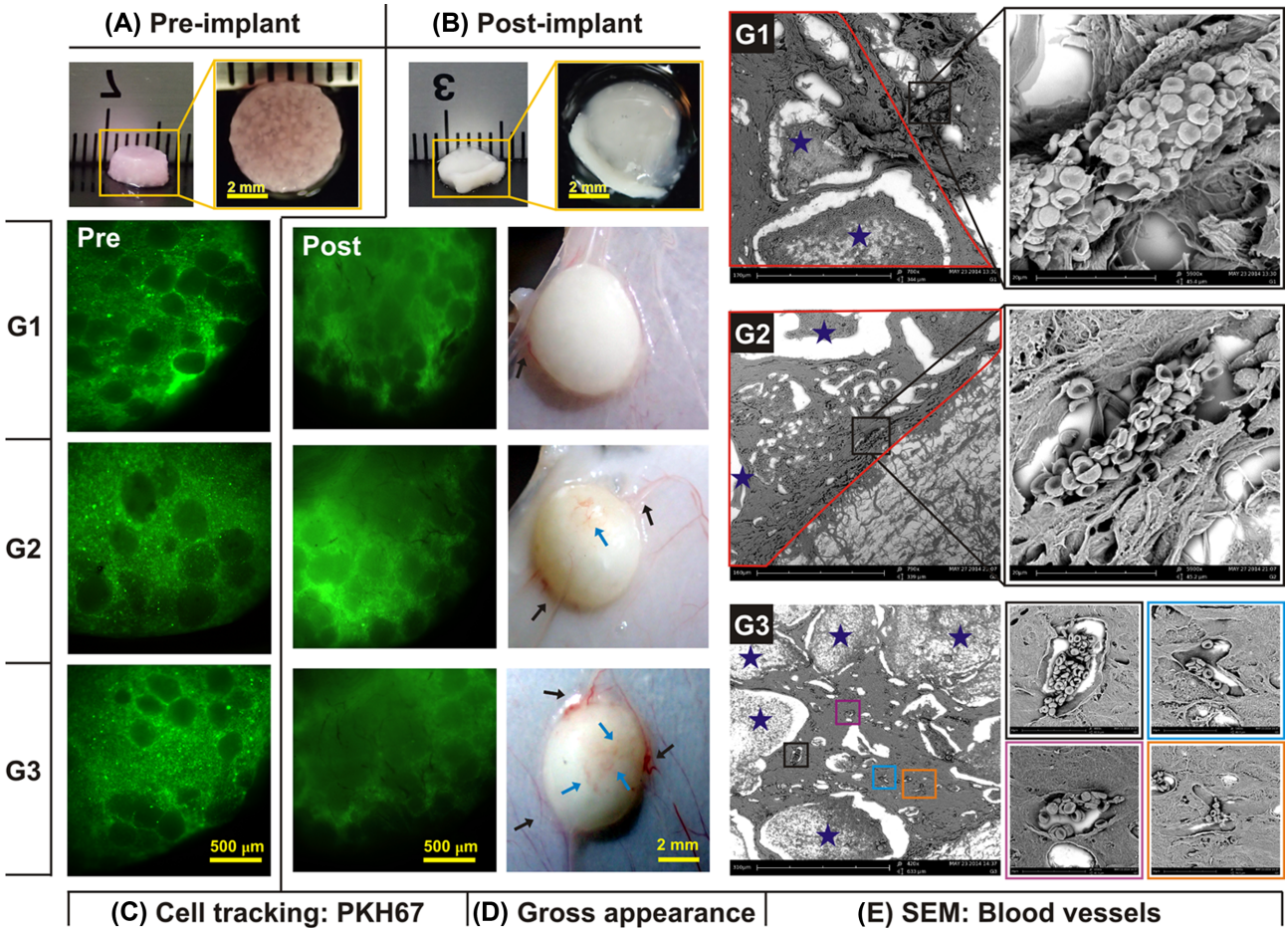

Figure 5. Subcutaneous transplantation of collagen/C-S MCs construct. Dual GF-loaded MCs were homogeneously mixed with 1% (w/v) collagen solution in ice bath to prevent the gelation of collagen, and followed by the addition of preosteoblasts (1×10^6). The constructs were subsequently transferred to 96-well plate and incubated at 37 ºC for 30 min to allow crosslinking of collagen. Three experimental groups were prepared: C-S MCs without GFs (G1), C-S MCs with single GF (BMP-2) (G2), and C-S MCs with dual GFs (G3). These constructs were incubated in an osteogenic medium for 24 h before subcutaneous implantation. Photographic image of collagen constructs containing MCs and preosteoblasts: (A) pre-transplantation and (B) post-transplantation. (C) PKH67 cell tracker (green) labeled images of constructs: pre-(left) and post-transplantation (right). (D) Gross appearance of the transplanted constructs after 3 weeks. (E) SEM images of 5 μm thin-sections of the constructs. Red line indicates the interface between host tissue and construct. MCs are marked in stars. Boxes in G3 are the sites of blood vessels formation inside the construct.

tion, finding an appropriate material that confers not only the capacity for such temporal delivery, but also high loading efficiency and biocompatibility is an equally imperative task.[27] Here, we demonstrate the *in vivo* feasibility of a platform, through which a collagen scaffold containing dual GF-loaded MCs and cells is subcutaneously implanted into the dorsal region of nude mice (Figure 5). More specifically, the effect of VEGF/BMP-2 temporal delivery on *in vivo* osteogenesis and angiogenesis is evaluated. Scaffolds prepared using temperature-sensitive rat tail collagen have a diameter of 5.5±0.3 mm and a thickness of 1.8±0.2 mm upon cross-linking (Figure 5(A)). Each construct contains C-S MCs, uniformly dispersed as white spheres and preosteoblasts. After incubation at 37 ºC for 24 h, the constructs are stained with a cell tracker dye PKH67 in order to examine the distribution and viability of the cells (Figure 5(C)-left); cells, which appear as green fluorescent dots, are homogenously distributed in the collagen region while C-S MCs, which appear as dark holes, are located in acellular regions of the construct. After subcutaneous implantation for 21 days, the retrieved constructs show that PKH67 still reserves some positive signals (Figure 5(C)-right). Preosteoblasts are distributed throughout the entire construct as indicated by the diffusion of the PKH67 signal, which points to the proliferation and migration of cells throughout the construct, including the interior of the C-S MCs. An examination of the constructs post-implantation reveals a reduction in construct size to a diameter of 5.0±0.3 mm and a thickness of 1.3±0.2 mm (Figure 5(B)). In gross appearance, vascular

recruitment is observed in all three groups (Figure 5(D)-black arrow); a higher degree of angiogenesis is observed in G3 than in G1 or G2, as confirmed by the penetration of a visible vascular network into the construct (Figure 5(D)-blue arrow). Furthermore, the formation of blood vessels was indirectly confirmed by analyzing thin sections of construct *via* SEM for the presence of red blood cells (RBCs) (Figure 5(E)). RBCs are present in the peripheral region of the construct at the interface (red line) between host tissue and construct; MCs are also observed (stars). A closer look reveals the presence of void space (white) surrounding the C-S MCs. It is interesting to note that compared to G1 and G2, the presence of RBCs in the center region of the collagen construct (G3) (Figure 5(E), inset) is apparent, and this is a strong indicative of deep penetration of host blood vessels inside the construct. This enhanced vascularization can be explained by the VEGF delivery in G3.

The implanted constructs are sectioned and stained with hematoxilin and eosin (H&E) for histological analysis (Figure 6). The collagen scaffold is distinguished by staining in pink red color and C-S MCs is spotted in white domain (Figure 6(A)). It is notable that many MCs are significantly swollen (denoted as a star) *in vivo*, whereas some MCs remain constant in their initial size (marked in triangle). The presence of blood cells is spotted in red color (Figure 6(A) insets, black arrow), indicating recruitment and penetration of blood vessels in and around the construct region. In addition to the formation of abundant blood vessels especially in G3, few inflammatory cells in all of the constructs are also noteworthy. In addition, ectopic calcification of the construct is evaluated *via von Kossa* staining (Figure 6(B)). More calcified nodules (black deposits) are observed in G2 and G3 than those in G1; a slightly higher amount of calcium deposits are detected in G3, compared to G2. Taken together, the designed construct can result in enhanced osteogenesis and angiogenesis while minimizing an inflammatory host response. The capacity of each group to induce *in vivo* osteogenesis and angiogenesis is also examined *via* IFS for osteocalcin (OCN) and α-smooth muscle actin (α-SMA), respectively (Figure 7). The results show minimal expression of OCN in G1 and an increased level of expression in G3 than in G2 (Figure 7(A)). When the OCN staining intensity is quantified *via* Image J (Figure 7(C)), a 5.8-fold and 8.2-fold increase in OCN expression is observed in G2 and G3, respectively, with respect to G1,

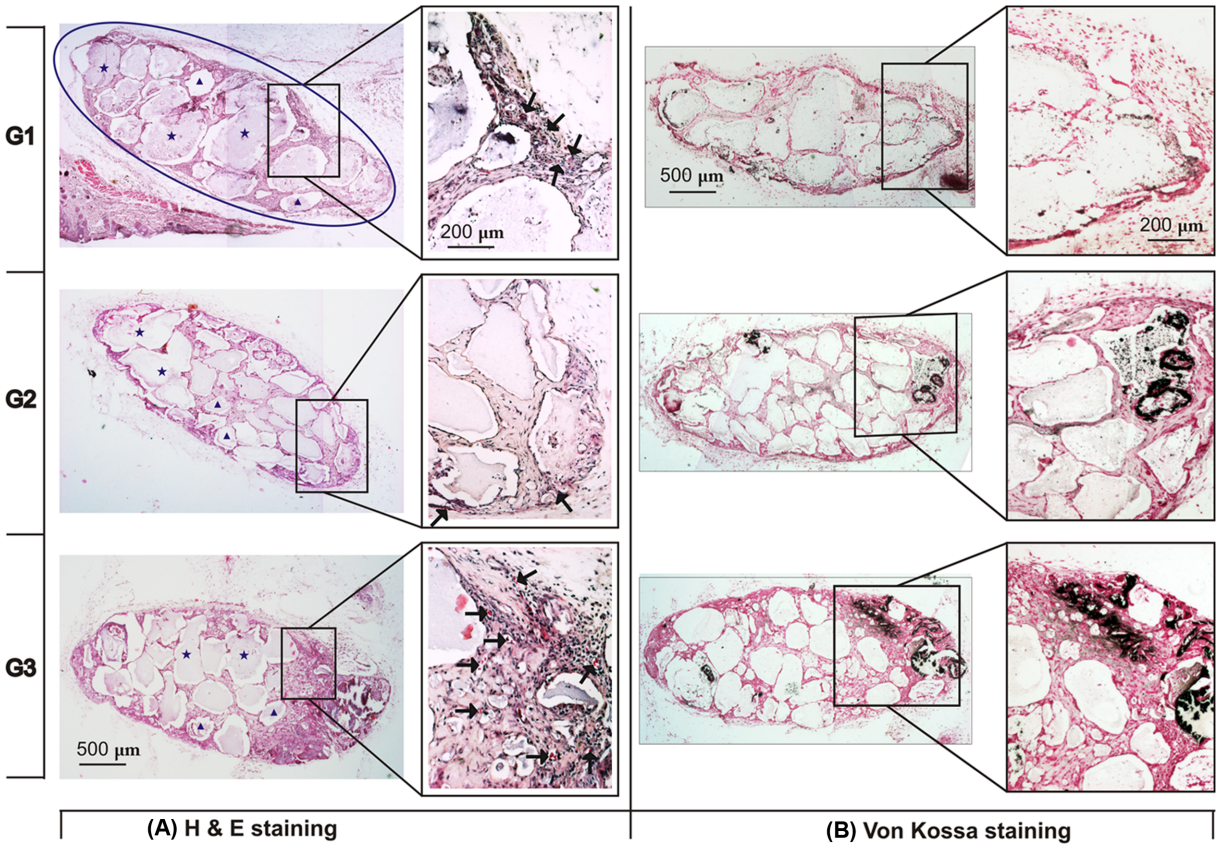

Figure 6. H&E and *von Kossa* staining of transplanted constructs. (A) H&E staining: Arrows indicate a sign of blood vessels formation: blood cells are stained in red. It is also notable that many MCs are significantly swollen (denoted as a star), whereas some MCs remain constant in their initial size (marked in triangle). (B) *Von Kossa* staining: Black stains are the calcified matrices co-stained with nuclear fast red.

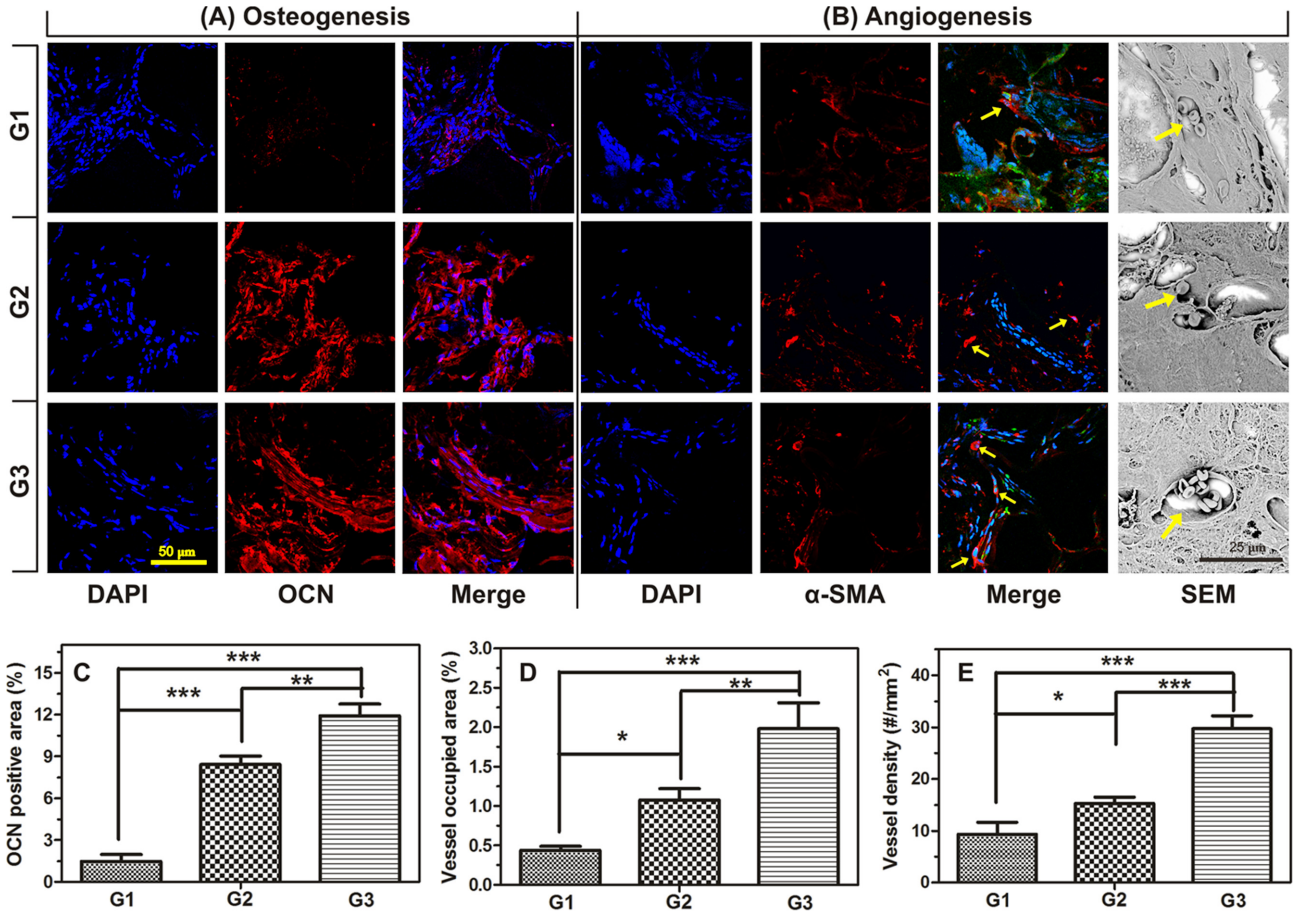

Figure 7. Osteogenic and angiogenic analysis of transplanted constructs. (A) IFS of osteogenic marker, OCN and (B) angiogenic marker, α-SMA, along with DAPI nuclear staining (blue), (C) percentage of OCN positive area, (D) percentage of vessel occupied area, and (E) measurement of vessel density. Statistical significance is marked as *(p<0.05), **(p<0.01), and ***(p<0.001).

which further supports dual GF delivery as a means to induce an enhanced level of ectopic osteogenesis. Additional data of α-SMA expression are similar to those for OCN (Figure 7(B)); the amount of smooth muscle cells lining the blood vessel (yellow arrows) indicate an enhanced level of α-SMA expression in G3 than in G2. Corresponding SEM images that detect RBCs in yellow arrow further corroborate this trend. Quantification of α-SMA signals exhibits a 2.4-fold and 4.5-fold upregulation in α-SMA expression for G2 and G3, respectively, with respect to G1 (Figure 7(D)). Similarly, quantification of total vessel area demonstrates a 1.6-fold and 3.2-fold rise in angiogenesis for G2 and G3, respectively, compared to G1 (Figure 7(E)).

This study demonstrates an increased level of osteogenesis and angiogenesis *via* dual delivery of BMP-2 and VEGF. In particular, *von kossa* staining and IFS suggest that BMP-2 alone (G2) prefers osteogenesis[28] as reported, whereas the dual delivery of BMP-2 and VEGF (G3) seems to contributes to improving both calcification and vascularization.[29] While numerous studies have documented the effect of dual GFs (mostly BMP-2/VEGF) on synergistic osteogenesis,[30] some conflicting reports argue that the level of osteogenesis *via* dual GF delivery is similar to that obtained *via* single BMP-2 delivery.[14,31] Nonetheless, preparation of a suitable carrier for the dual delivery of GFs is practically difficult and less reported. From these perspectives, we are able to fabricate C-S MCs for dual GF delivery and evaluate their synergistic effect on osteogenesis and angiogenesis using an all-in-one platform. Our *in vitro* and *in vivo* studies demonstrate that VEGF/BMP-2 delivery results in osteogenesis with an adequate vascular network in the construct. Future work using *in vivo* defect models would aid in elucidating the role of sequential or temporal delivery of GFs in the regeneration of vascularized bone.

Conclusions

In this study, we have investigated an optimal fabrication condition of C-S MCs preparation with regards to their size, shape, and loading efficiency. The dual GF-loaded MCs exhibited the release of BMP-2 from the alginate shell, followed by a

delayed release of VEGF from the core. The temporal release of BMP-2 from C-S MCs could induce osteogenesis of preosteoblasts *in vitro*. It is notable that the dual GF-loaded C-S MCs in conjunction with preosteoblasts and collagen were effective in advancing vascularization induced by a deep penetration of blood vessels *in vivo*. In summary, VEGF/BMP-2-loaded C-S MCs were successfully fabricated and their effects on both osteogenesis and angiogenesis were promising compared to single BMP-2 delivery.

Acknowledgments. This study was supported by the National Research Foundation and funded by the Ministry of Education, Science and Technology, Republic of Korea (2011-0028796). This work was also supported by an intramural grant (2E24680) of Korea Institute of Science and Technology (KIST).

References

(1) M. Mimeault, R. Hauke, and S. K. Batra, *Clin. Pharmacol. Ther.*, **82**, 252 (2007).
(2) M. P. Lutolf, P. M. Gilbert, and H. M. Blau, *Nature*, **462**, 433 (2009).
(3) M. P. Lutolf and J. A. Hubbell, *Nat. Biotechnol*., **23**, 47 (2005).
(4) R. E. Guldberg, H. A. Awad, G. Vunjak-Novakovic, H. Donahue, and A. Das, *IBMS BoneKEy*, **10**, 1 (2013).
(5) T. P. Richardson, M. C. Peters, A. B. Ennett, and D. J. Mooney, *Nat. Biotechnol.*, **19**, 1029 (2001).
(6) S. Kim, H. Rha, S. Surendran, C. Han, S. Lee, H. Choi, Y.-W. Choi, K.-H. Lee, J. Rhie, and S. Ahn, *Macromol. Res*., **14**, 565 (2006).
(7) W. Choi, Y. Kim, and G. Tae, *Macromol Res*., **19**, 639 (2011).
(8) H. Lim, H. Ghim, J. Choi, H. Chung, and J. Lim, *Macromol. Res*., **18**, 787 (2010).
(9) B. Jeon, S. Jeong, A. Koo, B.-C. Kim, Y.-S. Hwang, and S. Lee, *Macromol. Res*., **20**, 715 (2012).
(10) K. Lee, E. A. Silva, and D. J. Mooney, *J. R. Soc. Interface*, **8**, 153 (2011).
(11) D. H. Choi, R. Subbiah, I. H. Kim, D. K. Han, and K. Park, *Small*, **9**, 3468 (2013).
(12) Z. S. Patel, S. Young, Y. Tabata, J. A. Jansen, M. E. K. Wong, and A. G. Mikos, *Bone*, **43**, 931 (2008).
(13) C. A. Simmons, E. Alsberg, S. Hsiong, W. J. Kim, and D. J. Mooney, *Bone*, **35**, 562 (2004).
(14) D. H. R. Kempen, L. Lu, A. Heijink, T. E. Hefferan, L. B. Creemers, A. Maran, M. J. Yaszemski, and W. J. A. Dhert, *Biomaterials*, **30**, 2816 (2009).
(15) C. Borselli, H. Storrie, F. Benesch-Lee, D. Shvartsman, C. Cezar, J. W. Lichtman, H. H. Vandenburgh, and D. J. Mooney, *Proc. Natl. Acad. Sci. U.S.A.*, **107**, 3287 (2010).
(16) H. Park, J. S. Temenoff, Y. Tabata, A. I. Caplan, R. M. Raphael, J. A. Jansen, and A. G. Mikos, *J. Biomed. Mater. Res. A*, **88A**, 889 (2009).
(17) D. H. Choi, C. H. Park, I. H. Kim, H. J. Chun, K. Park, and D. K. Han, *J. Control. Release*, **147**, 193 (2010).
(18) S. Agarwal, J. H. Wendorff, and A. Greiner, *Polymer*, **49**, 5603 (2008).
(19) T. Nguyen, J. Lee, and J. Park, *Macromol. Res*., **19**, 370 (2011).
(20) G. Lee, J.-C. Song, and K.-B. Yoon, *Macromol. Res*., **18**, 571 (2010).
(21) R. Subbiah, M. Veerapandian, and K. S. Yun, *Curr. Med. Chem.,* **17**, 4559 (2010).
(22) Y. Lee, J.-B. Chang, H. K. Kim, and T. G. Park, *Macromol. Res*., **14**, 359 (2006).
(23) Y.-I. Jeong, D.-G. Kim, M.-K. Jang, J.-W. Nah, and Y.-B. Kim, *Macromol. Res*., **16**, 717 (2008).
(24) S.-W. Choi, S.-K. Moon, J.-Y. Chu, H.-W. Lee, T.-J. Park, and J.-H. Kim, *Macromol. Res*., **20**, 447 (2012).
(25) N. Rajan, J. Habermehl, M.-F. Cote, C. J. Doillon, and D. Mantovani, *Nat. Protoc*., **1**, 2753 (2007).
(26) D. Cun, D. K. Jensen, M. J. Maltesen, M. Bunker, P. Whiteside, D. Scurr, C. Foged, and H. M. Nielsen, *Eur. J. Pharm. Biopharm*., **77**, 26 (2011).
(27) K. A. Blackwood, N. Bock, and T. R. Dargaville, *Int. J. Polym. Sci*., **2012**, 25 (2012).
(28) J. M. Wozney, *Mol. Reprod. Dev*., **32**, 160 (1992).
(29) X. Song, S. Liu, X. Qu, Y. Hu, X. Zhang, T. Wang, and F. Wei, *Acta Biochim. Biophys. Sin*., **43**, 796 (2011).
(30) J. M. Kanczler, P. J. Ginty, L. White, N. M. Clarke, S. M. Howdle, K. M. Shakesheff, and R. O. Oreffo, *Biomaterials*, **31**, 1242 (2010).
(31) A. Khojasteh, H. Behnia, N. Naghdi, M. Esmaeelinejad, Z. Alikhassy, and M. Stevens, *Oral. Surg. Oral. Med. Oral. Pathol. Oral. Radiol.*, **116**, e405 (2013).